African Journal of Biotechnology Vol. 10(66), pp. 14968-14976, 26 October, 2011
Available online at http://www.academicjournals.org/AJB
DOI: 10.5897/AJB11.2305
ISSN 1684–5315 © 2011 Academic Journals

Full Length Research Paper

Expression and comparison of recombinant cholesterol oxidases (COD) in *Escherichia coli* with native cholesterol oxidase expressed in *Brevibacterium* sp.

Yu Xin[1]*, Hailin Yang[2], Xiaole Xia3, Ling Zhang[4], Yuran Zhang[5], Yanjun Tong[6], Yi Chen[7] and Wu Wang[8]

School of Biotechnology, Jiangnan University, Key Laboratory of Industry Biotechnology, Ministry of Education, Wuxi 214036, Jiangsu, P.R. China.

Accepted 28 September, 2011

The structure and bio-activity of an endogenous cholesterol oxidase from *Brevibacterium* sp. was compared to the same enzyme exogenously expressed in *Escherichia coli* BL21 (DE3) with and without N- or C-terminal his-tags. The different proteins were purified with affinity and subtractive protocols. The specific activity of the natural enzyme from *Brevibacterium* sp. was 17.5 ± 0.2 U/mg, while the activities of the exogenously expressed forms were 16 ± 0.3 U/mg for non-tagged enzyme from *E. coli*, 12 ± 0.1 U/mg for the N-terminal his-tagged enzyme, and 4 ± 0.3 U/mg for C-terminal his-tagged enzyme. Circular dichroism revealed that the added histidine residues altered the natural folding of the enzyme. The natural cholesterol oxidase was composed of 39% α-helix, 40% β-sheet, and 20% random coil, while the non-tagged enzyme was composed of 40% α-helix, 35% β-sheet, and 24% random coil. In contrast, the N-terminal his-tagged enzyme was composed of 45% α-helix, 29% β-sheet, and 25% random coil, and the C-terminal his-tagged enzyme was composed of 55% α-helix, 16% β-sheet, and 28% random coil. Hydrophobic fluorescence analysis revealed that the hydrophobicity of the enzyme was reduced by his-tags. Coenzyme-like fluorescent probe binding analysis indicated that the coenzyme binding site should be blocked by his-tags. The his-tag method for protein isolation can disrupt the catalytic activity of the cholesterol oxidase.

Key words: Cholesterol oxidase; *Brevibacterium* sp.; *Escherichia coli*; structural disruption, His-tags.

INTRODUCTION

Cholesterol oxidases are a group of FAD-dependent enzymes expressed and frequently secreted by micro-organisms, including *Brevibacterium* (Uwajima et al., 1974), *Streptomyces* spp. (Tomioka et al., 1976), *Corynebacterium* (Shirokano et al., 1977), *Arthrobacter* (Liu et al., 1983), *Pseudomonas* (Aono et al., 1994), and *Rhodococcus* (Kreit et al., 1994; Sojo et al., 1997). They have important industrial applications and are widely used for the determination of cholesterol in food and blood serum by peroxidase-coupled assays (Allain et al., 1974; Richmond 1992). In addition, they are used in the production of starting material for the chemical synthesis of pharmaceutical steroids.To produce cholesterol oxidases on a large scale, the genes were cloned, sequenced, and expressed in genetic engineering bacteria (Murooka et al., 1986; Ishizaki et al., 1989; Ohta et al., 1991). In our previous work, *Brevibacterium* sp. CCTCC M201008 was isolated from soil, and a cholesterol oxidase was expressed with the inducement of cholesterol (Lv et al., 2002); the COD gene was further cloned and expressed in *E.* coli (Wang and Wang, 2007).

To quickly purify proteins expressed in genetic engineering bacteria, affinity tags are linked at the N- or C-terminals of the target protein. The most common affinity tag is probably the his-tag, consisting of a short peptide of histidine residues that allow for convenient affinity chromatography using Ni-NTA columns (Porath, 1992). In many cases, however, the affinity tags actually disrupted the natural structure and reduced the functional

*Corresponding author. E-mail: marshalxy@gmail.com. Tel: +86 051085918119.

activity of the expressed proteins (Terpe, 2003).We developed an efficient protocol for one step of affinity chromatography of non-tagged cholesterol oxidases expressed in *E. coli* (Xin et al., 2011). In this research, natural cholesterol oxidases were purified from *Brevibacterium* sp. and from *E. coli*. The exogenously expressed enzyme was either non-tagged, N-terminal his-tagged, or C-terminal his-tagged. The structural and biological characteristics of these enzymes were systemically studied.

MATERIALS AND METHODS

Substrates and chemicals

Brevibacterium sp. M201008, obtained from the China Center for Type Culture Collection (CCTCC), was grown at 37°C in Luria-Bertani (LB) medium. The initial cloning of the cholesterol oxidase gene from *Brevibacterium sp.* M201008 was carried out in *E. coli* JM109 using the pGEM-T Easy vector (Promega, Madison, WI, USA). *Escherichia coli* BL21-CodonPlus (DE3)-RP (Novagen, USA) was also used as host for the expression of the cholesterol oxidase gene from the *Brevibacterium* sp. via the T7 RNA polymerase expression system with pET-28a plasmid (Novagen). Cyanogen bromide (CNBr) was from Sigma (USA), Sepharose 4B was from Pharmacia Biotech (Sweden), and 8-anilinonaphthalene-l-sulfonic acid (ANS) was from Sigma-Aldrich. All other chemicals were of analytical grade and were from local companies.

Purification of cholesterol oxidase from *Brevibacterium* sp. M201008

Brevibacterium sp. M201008, preserved by our laboratory, was cultured according to our previously described methods (Lv et al., 2002). After cultivation, samples of culture were centrifuged at 7000 rpm (4°C), and then the natural cholesterol oxidase was purified from the cell-free extract using an affinity column (Xin et al., 2011). The purified enzyme was stored at -70°C for further analysis.

Expression of cholesterol oxidase gene in *E. coli*

The pET-28a-*choBb* plasmid containing the cDNA of cholesterol oxidase cloned in vector pET-28a (+) was described in our previous work (Wang and Wang, 2007). For expression of the mature *choB* gene, pET-*choB*$_m$ was constructed by cloning the *choB* gene into pET28a.

For non-tagged cholesterol oxidase, the forward primer 5'-AATTACCgCCATggCCCCCAgCCgCACCCTC-3' (Primer 1) was designed with a *Nco* I restriction site (underlined) and the reverse primer 5'-AATTACCgAAgCTTTCACTggATgTCggACgAgATg- 3' (Primer 2) was designed with a *Hind* III restriction site (underlined).

For N-terminal his-tagged cholesterol oxidase, the forward primer 5'-AATTACCggAATTCgCCCCCAgCCgCACCCTC-3' (Primer 3) was designed with an *Eco*R I restriction site (underlined) and Primer 2 was used as reverse primer.

For C-terminal his-tagged cholesterol oxidase, Primer 1 was employed as the forward primer and the reverse primer 5'-AATTACCgAAgCTTCTggATgTCggACgAgATg-3' (Primer 4) was designed with a *Hind* III restriction site (underline nucleotides).

The complete coding region of the mature *Brevibacterium* sp. DGCDC-82 *choB* was amplified by PCR using the plasmid pET-28a-*choBb* as the template. The PCR product was digested with the appropriate restriction enzyme pair before it was cloned into the same enzyme site in the pET-28a (+) vector. The *choB*$_m$ gene was expressed under the strong *trp/lac* promoter induced by IPTG.*E. coli* BL21 (DE3), harboring the pET28a-choB$_m$, was grown at 37°C overnight in LB medium containing kanamycin (20 µg/ml). The culture was then transferred into 100 ml of LB medium with the same antibiotic concentration and cultivated at 37°C until the OD_{600} reached 2. Gene expression was then induced with 0.8 mM IPTG for 10 h at 23°C. The cells were harvested by centrifugation at 6,000 rpm for 20 min at 4°C and re-suspended in 20 mM sodium phosphate buffer (pH 7.2). The cells were disrupted by sonication and centrifuged at 10,000 rpm for 30 min at 4°C. The supernatant was then assayed for enzyme activity. The protein concentrations were determined by the Lowry method using bovine serum albumin as the standard.

Purification of cholesterol oxidases expressed in *E. coli*

The non-his-tagged cholesterol oxidase was purified using an affinity column (Xin et al., 2011). However, the two his-tagged enzymes could not bind tightly to the affinity medium. Furthermore, the C-terminal his-tagged enzyme could not even be captured by the Ni-NTA column; therefore, a subtractive protocol (Shao et al. 2011) was employed for the purification of the two his-tagged enzymes.

Polyclonal antibodies were raised against total proteins extracted from non-plasmid *E. coli* BL21 (DE3) using standard methods (Bailey 1994). The rabbit serum was tested for reactivity to *E. coli* proteins by enzyme-linked immunosorbent assay (ELISA), and then harvested when the immunization titer reached 10^6. The antibodies were separated with a Protein A column, dialyzed against 0.1 M Na_2CO_3-$NaHCO_3$ (pH 8.0), and then coupled to CNBr activated Sepharose CL 4B using standard methods (David, 1974).

A 20 ml sample of the supernatant of disrupted *E. coli* was mixed with 20 ml equilibrating buffer (20 mM sodium phosphate, pH 7.2, 3 mS/cm). A 1 ml sample of the mixture containing about 2 mg total proteins was mixed with ~ 2 ml of the equilibrated antibody medium and then mixed at 4°C for 2 h. After centrifuged at 3,000 rpm for 10 min, his-tagged enzymes remained in the supernatant. The concentrations of proteins were determined by the Lowry Method using bovine serum albumin as the standard.

SDS-PAGE analysis

Reducing SDS-PAGE (12.5%) analysis was carried out on a Mini-protean II system from Bio-Rad (Hercules, CA, USA). For gel electrophoresis, 10 µl samples were mixed with 10 µl loading buffer (2% SDS, 350 mM DTT, 25% (v/v) glycerol, 0.01% Bromophenol Blue in 62.4 mM Tris–HCl, pH 6.8) and incubated at 95°C for 5 min before loading. Proteins were separated on 12.5% SDS-polyacrylamide gels. Gels were stained with Coomassie Brilliant Blue R, destained, and imaged using Gelpro Analyzer 3.0 software (Media Cybernetics, Inc.) for analysis of purity and molecular mass. The purity on reducing SDS-PAGE (12.5%) gels was calculated by integration of the lane darkness.

Cholesterol oxidase bioactivity assay

Cholesterol oxidase activity was assayed by quantifying the H_2O_2 produced from the coupling reaction with horseradish peroxidase (0.01 mg/ml) and aminopyrine. One unit of cholesterol oxidase activity was defined as the formation of 1 µmol H_2O_2 per min at 37 °C (Richmond, 1973; Ji, 2000). The K_m and V_{max} were estimated from Lineweaver–Burk plots of data obtained with assay solutions containing from 0 to 1 mM cholesterol.

Purified proteins (10 µg) were dissolved in each of the following solutions: 20 mM sodium acetate/acetic acid buffer (pH 5.0), 20 mM

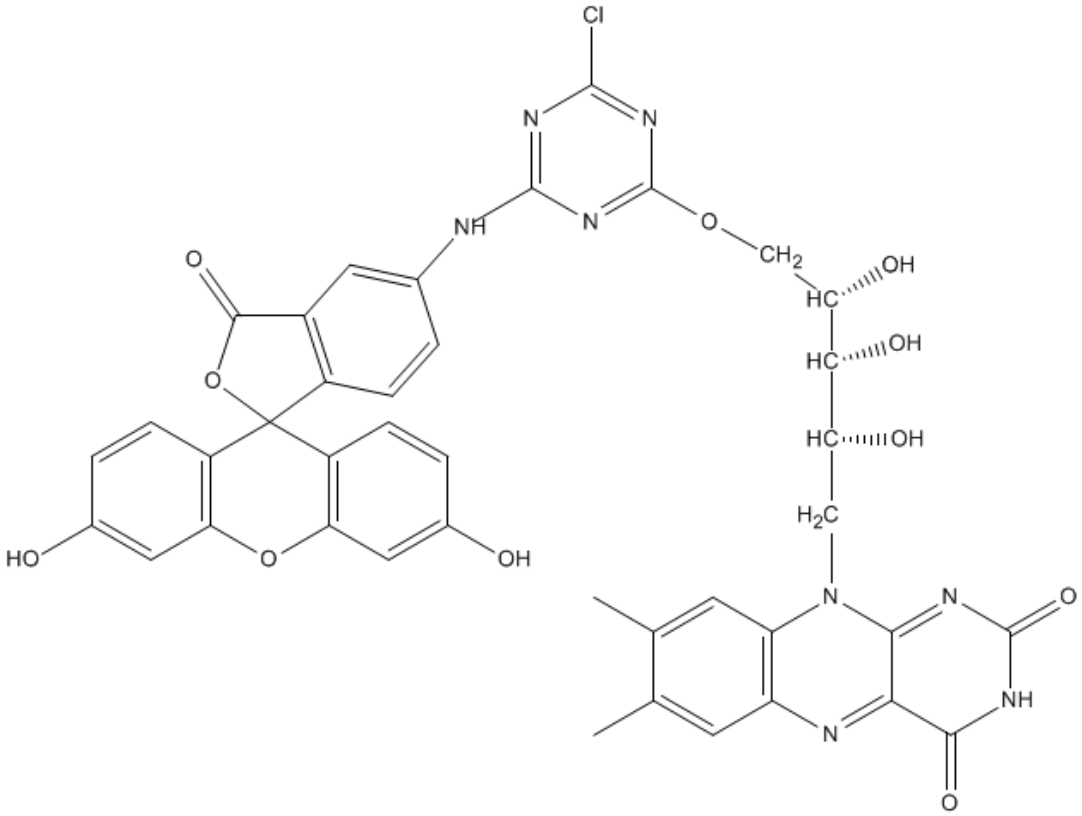

Figure 1. Chemical structure of the fluorescent probe RF-CC-AF.Riboflavin is linked to 5-aminofluorescein via cyanuric chloride.

sodium phosphate buffer (pH 6.0 and 7.0), 20 mM Tris/HCl buffer (pH 8.0), 20 mM glycine/NaOH buffer (pH 9.0 and 10.0), or NaOH (pH 11.0). The samples were incubated at 37°C for 2 h and then subjected to bioactivity assays.

Purified proteins (10 µg) were dissolved in 20 mM sodium phosphate buffer (pH 7.0) incubated at 15, 20, 25, 30, 35, 40, 45, 50, 55, 60, or 65°C for 2 h and then tested for bioactivity at the same (incubation) temperature.

CD spectroscopy

The CD spectrum of 0.2 mg/ml (pH 7.0, 25°C) purified protein was scanned with a Jasco J-715 spectropolarimeter in a cell with a path length of 1 mm (Slade et al., 2005). The CD spectrum was measured from 190 to 250 nm. The data from triplicate measure-ments were averaged and then submitted to the K2d online server (http://www.embl-heidelberg.de/~andrade/k2d.html) in order to estimate the percentages of different secondary structures.

Hydrophobic-pocket analysis using ANS

The fluorescent dye ANS can interact with hydrophobic pockets of proteins, and this interaction induced changes in the molecule's fluorescence intensity (Schönbrunn et al., 2000). The four purified enzymes (2 µM) were mixed with 100 µM ANS and dissolved in each of the following solutions: 20 mM sodium acetate/acetic acid buffer (pH 5.0), 20 mM sodium phosphate buffer (pH 6.0 and 7.0), 20 mM Tris/HCl buffer (pH 8.0), 20 mM glycine/NaOH buffer (pH 9.0 and 10.0), and NaOH solution (pH 11.0). The resulting mixtures were incubated for 60 min at 25°C, and the 485 nm emission of each solution was measured at a $\lambda_{excitation}$ of 355 nm with a Fluoroskan Ascent fluorimeter (LabSystems, Helsinki, Finland). The fluore-scence intensities of ANS solutions in the absence of protein served as baseline controls and were subtracted from the spectra of the ANS or protein mixtures. The dye dissociation constant (K_d) was indicative of the strength of the ANS–protein interaction and was calculated using

$$y = y_{\max} \times [ANS] / (K_d + [ANS])$$

Where y is the observed fluorescence signal, y_{max} is the maximal fluorescence signal observed, and [ANS] is the concentration of ANS.

Synthesis of fluorescent probe and FAD binding site analysis of the protein

A fluorescent probe synthesized from riboflavin, cyanuric chloride, and 5-aminofluorescein, termed 'RF-CC-AF' (Figure 1), was produced by the method of Li et al. (1998).

Purified protein (2 µM) was dissolved in each of the following solutions: 20 mM sodium acetate or acetic acid buffer (pH 5.0), 20 mM sodium phosphate buffer (pH 6.0 and 7.0), 20 mM Tris/HCl buffer (pH 8.0), 20 mM glycine/NaOH buffer (pH 9.0 and 10.0), and NaOH solution (pH 11.0). The resulting solutions were each mixed with a 2 µM solution of fluorescent probe and incubated for 60 min at 25°C. The fluorescence emission at 527 nm was measured in response to 485 nm $\lambda_{excitation}$ using a Fluoroskan Ascent fluorimeter

Table 1. The recoveries of the purification processes.

Parameter	Step	Protein		Activity		
		mg	Yield (%)	Total activity (U)	Specific activity (U/mg)	Yield (%)
Natural enzyme	Crude sample	302 ± 7.55	100	697.5 ± 12.6	2.3 ± 0.2	100
	Affinity purification	36.5 ± 6.35	12.1	638.8 ± 10.3	17.5 ± 0.2	91.6
Non-tagged enzyme	Crude sample	252 ± 5.5	100	335 ± 11.5	1.33 ± 0.1	100
	Affinity purification	20 ± 0.45	7.9	320 ± 6.5	16 ± 0.3	95.5
N-terminal-tagged enzyme	Crude sample	2 ± 0.10	100	4.6	2.3 ± 0.2	100
	Subtractive purification	0.26 ± 0.02	13.0	3.12	12 ± 0.1	67.8
C-terminal-tagged enzyme	Crude sample	2 ± 0.10	100	1.4	0.7 ± 0.1	100
	Subtractive purification	0.2 ± 0.02	10.0	0.8	4 ± 0.3	57.1

(Labsystems). The fluorescence spectra of the RF-CC-AF solutions in the absence of protein were used as baseline controls and subtracted from the corresponding RF-CC-AF-protein spectra.

RESULTS

Preparation of cholesterol oxidases

After centrifuged at 7000 rpm (4℃), the native cholesterol oxidase of *Brevibacterium* sp. M201008 was extracted from the supernatant of the cultures and further adjusted to an affinity column equilibrated with 20 mM sodium phosphate pH 7.2). After washing with 20 mM sodium phosphate/0.02M NaCl (pH 7.2), the enzyme was eluted by 20 mM sodium phosphate/0.3M NaCl (pH 7.2) with high purity. The purified enzyme was stored at -70℃ for further analysis.

The non-his-tagged enzyme expressed in *E. coli* was purified according to our previous method (Xin et al., 2011).

For the two his-tagged enzymes, supernatants of disrupted *E. coli* were adjusted to pH 7.2 and further mixed with equilibrated affinity medium. After centrifuged, the two enzymes remained in the supernatants. The protein yields of the four enzymes are listed in Table 1.

SDS-PAGE analysis

In reducing SDS-PAGE (12.5%) analysis, all four forms of the enzyme demonstrated almost the same single band at ~ 50 kDa. The calculated purities were about 98.5, 97.3, 95.5, and 95.5% respectively, (Figure 2).

Bioactivity assay of purified enzyme

The specific activity of natural enzyme from *Brevibacterium* sp. was 17.5 ± 0.2 U/mg and that of the non-his-tagged enzyme expressed in *E. coli* was 16 ± 0.3 U/mg. The N-terminal his-tagged enzyme and C-terminal his-tagged enzyme had markedly lower activities of 12 ± 0.1 and 4 ± 0.3 U/mg, respectively. The activity recoveries of the purification processes are listed in Table 1.

The K_m and V_{max}, estimated from Lineweaver–Burk plots using 0 to 1 mM cholesterol, were 24.3 μM and 26.5 μmol min^{-1} mg^{-1} of protein for the native enzyme from *Brevibacterium* sp. M201008; 25.4 μM and 24.2 μmol min^{-1} mg^{-1} of protein for the non-his-tagged enzyme expressed in *E. coli.* The N-terminal his-tagged enzyme showed K_m at 35.4 μM and V_{max} at 18.5 μmol min^{-1} mg^{-1} of protein, while equivalent values for the C-terminal his-tagged enzyme were 45.2 μM and 6.2 μmol min^{-1} mg^{-1} of protein (Table 2).

Stability analysis

The cholesterol oxidase activities of the four purified proteins at 37℃ demonstrated the expected bell-shaped pH dependence with maxima at pH 7.0 (Figure 3A). Below pH 5.0 and above pH 11.0, however, each form of the enzyme had very low activity. The optimal reactive temperature of each protein was 35 to 40℃ (Figure3B).

CD analysis of secondary structure

The CD spectra of the purified enzymes were obtained at pH 7.0 and 25℃. Data between 190 nm and 250 nm was typically deemed credible. The K2d online server was used to predict the molecule's secondary structure. The natural cholesterol oxidase was composed of 39% α-helix, 40% β-sheet, and 20% random coil, while the non-tagged enzyme was composed of 40% α-helix, 35% β-sheet, and 24% random coil. In contrast, the secondary structures of his-tagged enzymes were apparently different. The

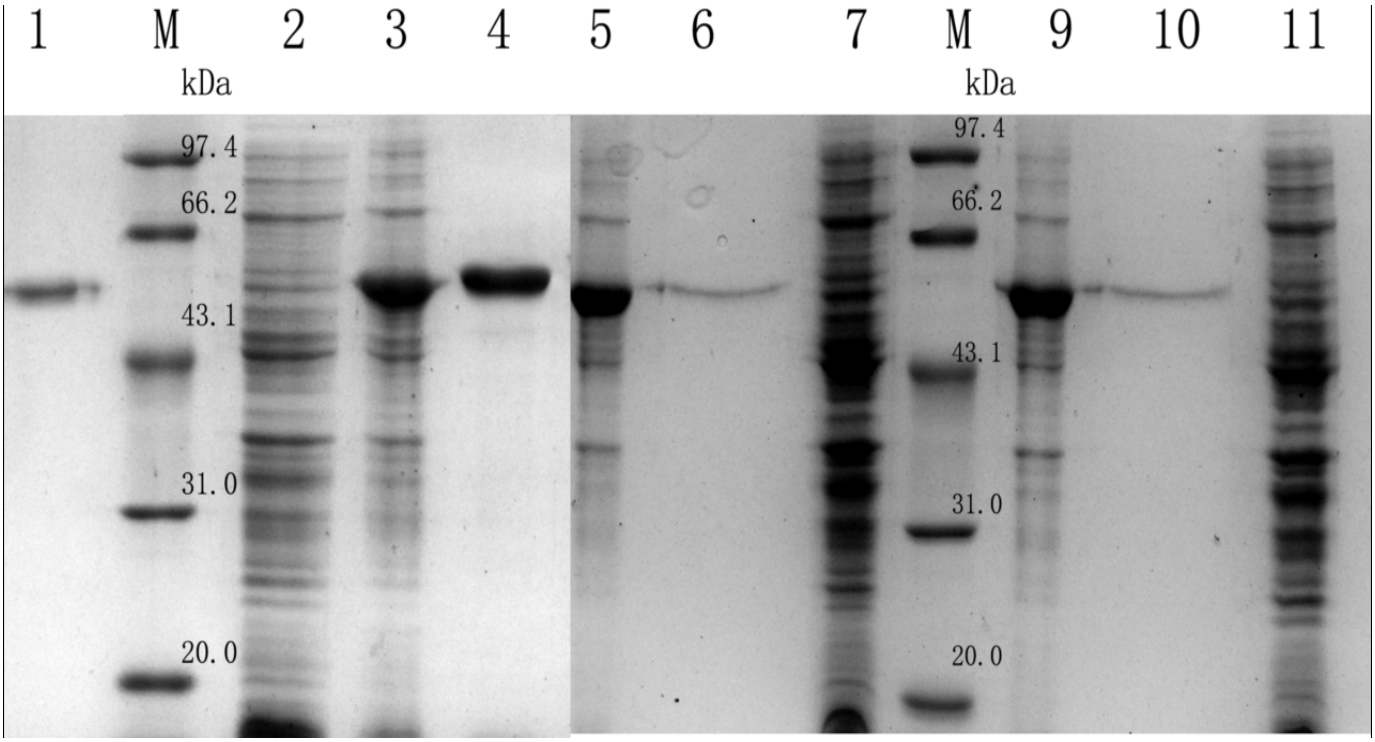

Figure 2. SDS analysis of purified enzyme. Lan M was molecular marker; Lane 1 was the natural cholesterol oxidases purified from *Brevibacterium* sp. M201008; lane 2 was the total proteins extracted from non-plasmid bearing E. *coli*; lane 3 was the total proteins of E. *coli* expressing non-his-tagged enzyme; lane 4 was the non-his-tagged enzyme expressed in E. *coli*; lane 5 was the total protein extracted from *E. coli* cells expressing N-terminal-his-tagged enzyme; lane 6 was the flow through fraction including N-terminal-his-tagged enzyme; lane 7 was the eluted cell back ground proteins; lane 8 was the total protein extracted from *E. coli* cells expressing C-terminal-his-tagged enzyme; lane 9 was the flow through fraction including C-terminal-his-tagged enzyme; lane 10 was the eluted cell back ground proteins.

N-terminal his-tagged enzyme was composed of 45% α-helix, 29% β-sheet, and 25% random coil, while the C-terminal his-tagged enzyme contained 55% α-helix, 16% β-sheet, and 28% random coil (Figure 4).

Hydrophobic-pocket analysis with ANS

Under acidic (pH 5.0, 6.0), neutral (pH 7.0) and alkaline (pH 8.0, 9.0, 10.0, 11.0) conditions, the fluorescence intensity of ANS in the presence of the enzymes is presented as:

$$y = y_{\max} \times [ANS] / (K_d + [ANS])$$

This indicated that the natural enzyme probably contained a single hydrophobic pocket suitable for ANS binding. The maximal fluorescent intensities (y_{max}) and the dissociation constants (K_d) of ANS–protein interaction for the four enzymes are listed in Table 3.

The pH-dependence of the ANS–enzyme interaction was also bell shaped (Figure 5A), indicating that the hydrophobicity of the pocket was at its lowest under acidic conditions. As the pH increased, the hydrophobicity of the pocket gradually increased to peak at pH 7.0. The quickly decreasing pocket hydrophobicity above pH 10.0 should be attributed to the degradation of the pocket's structural integrity.

Coenzyme binding site analysis with fluorescent probe

Flavoenzymes usually contained a coenzyme binding site and the binding of co-enzyme (FAD or FMN) are critical for the bioactivities of these enzymes. In our previous work, according to Xin et al. (2011), the purified cholesterol oxidase could not covalently bind FAD, but still had cholesterol oxidation activity without the cooperation of FAD.

A fluorescent probe was synthesized, RF-CC-AF, which can recognize the cholesterol oxidases coenzyme binding site. Once bound to the enzyme, variations in the fluorescence intensity of the probe were measured at different pH values (Figure 5B). The fluctuations in fluorescence should be attributed to conformational changes within the coenzyme binding site, and the variations in enzyme-probe interactions. At low pH (pH 5.0), the variations in fluorescence were small, indicating that the coenzyme binding site could hardly bind with the probe. As the pH increased, however, the fluctuations in fluorescence

Table 2. The constants for the bioactivity of the four enzymes.

Parameter	K_m (μM)	V_{max} (μmol min^{-1} mg^{-1})
Natural enzyme	24.3	26.5
Non-tagged enzyme	25.4	24.2
N-terminal histagged enzyme	35.4	18.5
C-terminal histagged enzyme	45.2	6.2

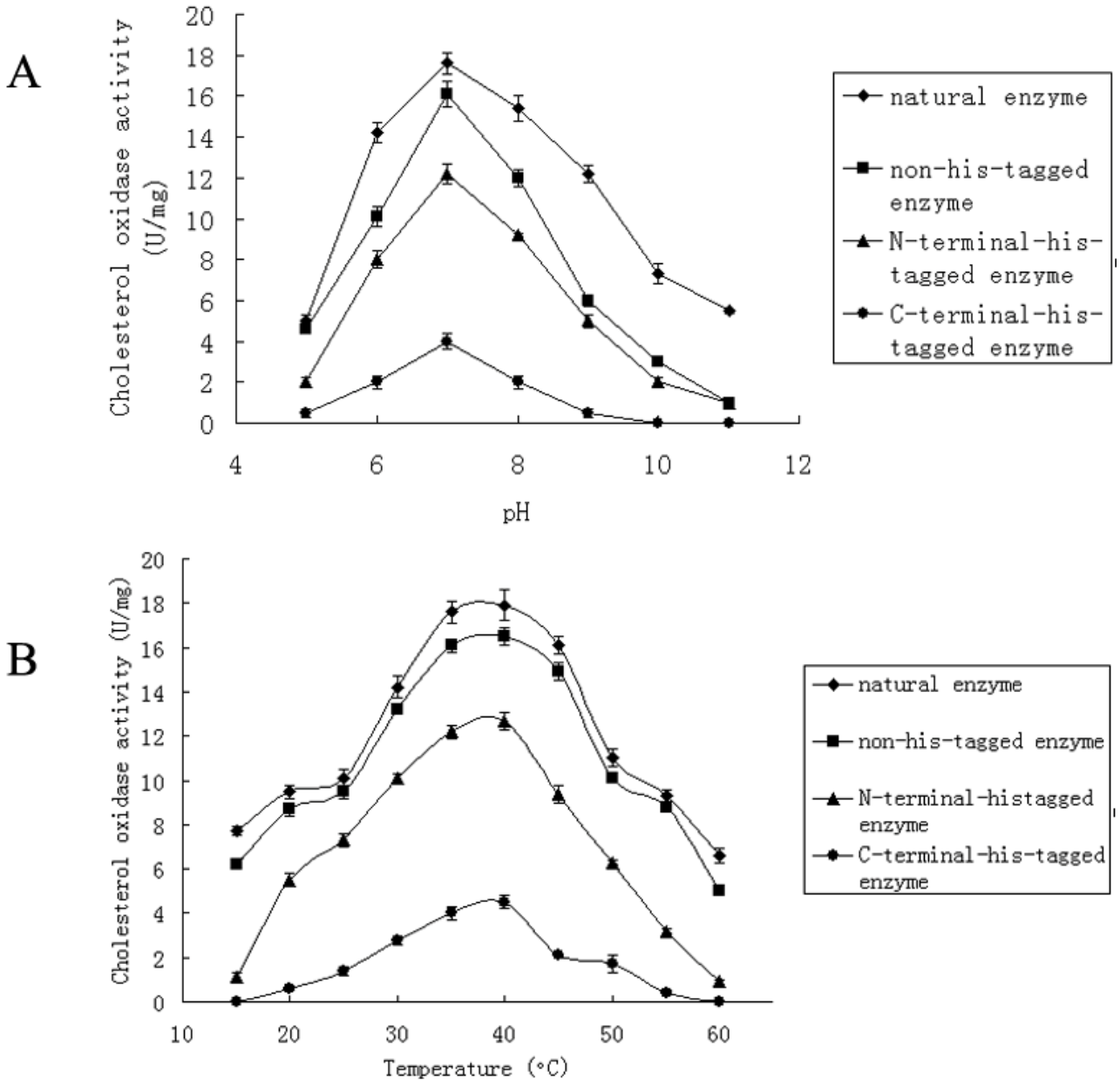

Figure 3. The optimal pH and temperature of four cholesterol oxidases**.** The opti.mal pH of four purified enzymes and standard were all at ~7.0;The optimal temperatures of four purified enzymes and standard were all at 35 to 40℃.

intensity also increased, and were highest at pH 7.0, indicating that the increase in pH enhanced the enzyme-probe interaction. The fluctuations in fluorescence decreased again at pH values above 9.0, possibly due to

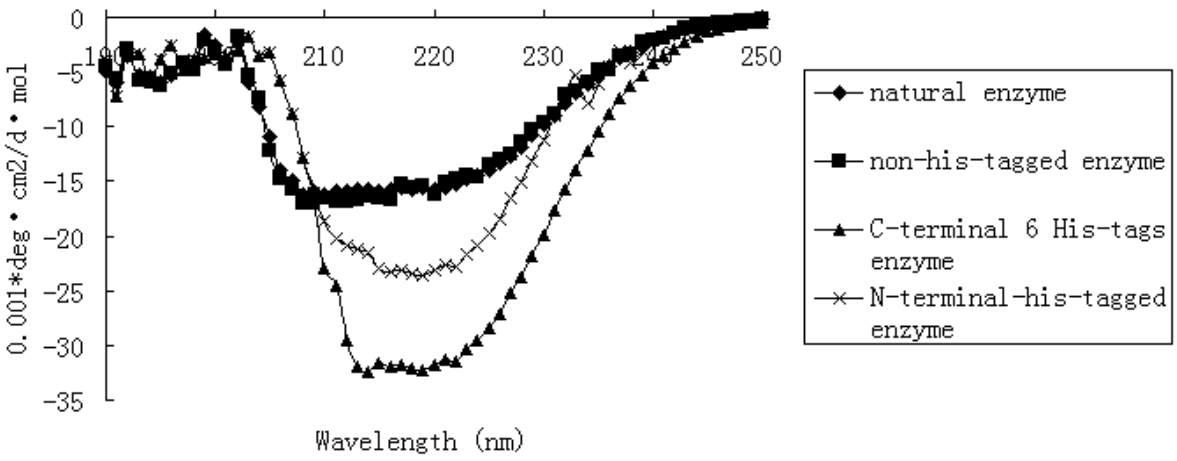

	α-helix (%)	β-sheet (%)	random coil (%)
natural enzyme:	39	40	20
non-his-tagged enzyme:	40	35	24
N-terminal-his-tagged enzyme:	45	29	25
C-terminal-his-tagged enzyme:	55	16	28

Figure 4. The secondary structure analysis. The secondary structures of the four enzymes were predicted with CD spectra.

Table 3. The maximal fluorescent intensities (y_{max}) and the dissociation constants (K_d) of ANS–protein interaction.

Parameter	pH 5		pH 6		pH 7		pH 8		pH 9		pH 10	
	y_{max}	K_d (μM)	y_{max}	K_d (μM)	y_{max}	K_d (μM)	y_{max}	K_d (μM)	y_{max}	K_d (μM)	y_{max}	K_d (μM)
Natural enzyme	2.45	273.3	3.43	236.5	9.31	146.7	4.62	199.6	3.41	218.6	2.11	279.9
Non-tagged enzyme	2.24	280.1	3.21	239.2	8.99	150.4	4.36	207.6	3.18	222.3	1.99	287.6
N-terminal histagged enzyme	1.67	320.1	2.29	299.7	6.16	218.2	3.22	265.4	2.37	289.1	1.39	331.3
C-terminal histagged enzyme	0.51	663.2	0.87	605.6	2.32	522.3	1.21	586.4	0.88	626.5	0.52	680.1

structural breakdown of the protein or complete dissociation of the probe from the active site.

DISCUSSION

The secondary structure and catalytic activity of the cholesterol oxidase from *Brevibacterium* sp. M201008 was compared to the same enzyme expressed in *E. coli* BL21 (DE3) with and without his-tags on the C- or N-terminal. In the purification process, natural and non-his-tagged enzymes could be efficiently captured by an affinity medium based on flavo-coenzyme (Xin et al., 2011); conversely, N- and C-terminal his-tagged cholesterol oxidases did not bind with the coenzyme-like affinity ligand, suggesting that coenzyme binding was affected by his-tags. Furthermore, the N-terminal his-tagged enzyme could be captured by a Ni-NTA column, with the

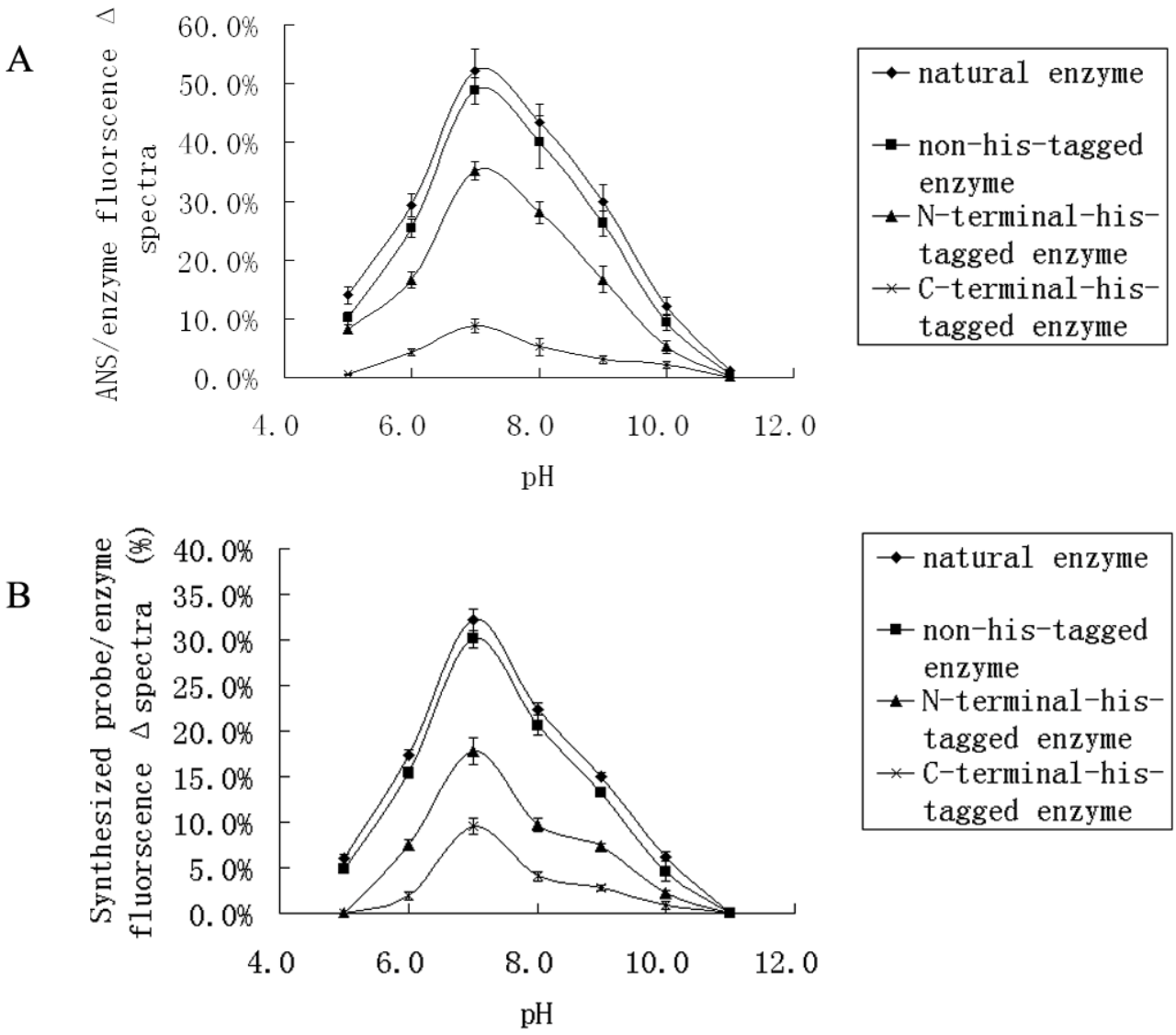

Figure 5. The fluorescent analysis of the enzymes: (A) Hydrophobic-site analysis using ANS: variations in the fluorescence of protein-bound AND at different pH values ($\lambda_{excitation}$ 355 nm and $\lambda_{emission}$ 485 nm). (B) Coenzyme binding site analysis using the fluorescent probe RF-CC-AF: variations in the fluorescence of the protein-bound probe at different pH values ($\lambda_{excitation}$ 485 nm and $\lambda_{emission}$ 527 nm.

C-terminal his-tagged enzyme all flew through the medium.

Additionally, the non-tagged enzyme expressed in *E. coli* showed quite different structural and enzymatic properties from other two his-tagged enzymes while retaining almost the same specific activity and bio-reaction constants as the natural enzyme. Indeed, the his-tagged forms were distinct structurally and biochemically, especially the C-terminal his-tagged enzyme, which exhibited less than 25% of the native enzyme bioactivity.

Secondary structure analysis reflected that the non-tagged cholesterol oxidase shared almost the same α-helix and β-sheet contents with natural enzyme, followed by his-tagged enzyme with dramatically declined β-sheet contents, especially in the C-terminal his-tagged form. It was previously reported that in the case of *Brevibacterium* cepacia ST-200 cholesterol oxidase, the α-helix content significantly increased while the β-sheet and the natural bioactivity were rapidly lost when the temperature was quickly increased (Doukyu et al., 2009). In our experiment, addition of the his-tags should disintegrate the β-sheet structures which were vital for the bio-function of flavoenzymes.

Comparing the data from the coenzyme binding site analysis, hydrophobic-pocket analysis and bioactivity assays, we observed similar trends in response to changes in pH. It was interesting that the greatest hydrophobicity of the enzymes was detected at pH 7.0,

followed with highest coenzyme binding abilities and cholesterol degradation activities. Specifically, this suggested that the hydrophobic pocket was closely associated with the coenzyme binding site.

To efficiently purify proteins expressed in genetic engineering bacteria, his-tags are often employed with metal-chelating chromatography. However, these tags can alter the natural folding of proteins and interfere with bioactivity. Furthermore, his-tags are sometimes packaged into the proteins and locate under the protein surface, precluding metal-chelating chromatography.

ACKNOWLEDGEMENTS

This work was supported by a grant from the National High Technology Research and Development Program of China (863 Program) (No. 2006AA10Z305), Program of the Science and Technology Support Plan of Jiangsu Province (No. SBE201077545 and SBE201170578), Scientific Research Program of the Cross Creative Team of Jiangnan University (No. JUSRP30904), Scientific Research Foundation for Young Scholars of Jiangnan University (No.2009LQN03), the program of the Key Laboratory of Industrial Biotechnology, Ministry of Education, China (No. KLIB-KF200906), Scientific Program of Jiangnan University (No. JUSRP11120).

REFERENCES

Allain CC, Poon LS, Chan CSG, Richmond W, Fu PC (1974). Enzymatic determination of total serum cholesterol. Clin. Chem. 20: 470–475.

Aono R, Doukyu N, Kobayashi H, Nakajima H, Horikoshi K (1994). Oxidative bioconversion of cholesterol by *Pseudomonas sp.* strain ST-200 in a water-organic solvent two-phase system. Appl. Environ. Microbiol. 60: 2518–2523.

Bailey GS (1994). The raising of a polyclonal antiserum to a protein. Methods. Mol. Biol. 32: 381-388.

David GS, Chino TH, Reisfeld RA (1974). Binding of proteins to CNBr-activated Sepharose 4B. FEBS Lett. 43 (3): 264-266.

Doukyu N, Shibata K, Ogino H, Sagermann M (2009). Cloning, sequence analysis, and expression of a gene encoding *Chromobacterium* sp. DS-1 cholesterol oxidase. Appl. Microbiol. Biotechnol. 82: 479-490.

Ishizaki T, Hirayama N, Shinkawa H, Nimi O, Murooka Y (1989). Nucleotide sequence of the gene for cholesterol oxidase from a *Streptomyces* sp. J. Bacterol. 171: 596–601.

Ji WM (2000). Production and properties of cholesterol oxidase from Brevidbacterium sp, PhD dissertation, Wuxi Univeristy of Light Industry, Wuxi, China.

Kreit J, Lefebvre G, Germain P (1994). Membrane-bound cholesterol oxidase from Rhodococcus sp. cells; production and extraction. J. Biotechnol. 33: 271–282.

Li R, Dowd VD, Stewart J, Burton SJ, Lowe CR (1998). Design, Synthesis and Application of an Artificial Protein A. Nat. Biotechnol. 16(2): 190-195.

Liu W, Hsu J, Wang W (1983). Production of cholesterol oxidase by antibiotic resistant mutant and a constitutive mutant Arthrobacter simplex B-7. Proc. Natl. Sci. Counc. ROC. 7: 255–260.

Lv CF, Wang W, Tang YX, Wang LG (2002). Effect of cholesterol bioavailability- improving factors on cholesterol oxidase production by a mutant *Brevibacterium* sp. DGCDC-82. Process Biochem. 37: 901–907

Murooka Y, Ishizaki T, Nimi O, Maekawa N (1986). Cloning and expression of a Streptomyces cholesterol oxidase gene in Streptomyces lividans with plasmid plJ702. Appl. Environ. Microbiol. 52: 1382–1385

Ohta T, Fujishiro K, Yamaguchi K, Tamura Y, Aisaka K, Uwajima T (1991). Sequence of gene choB encoding cholesterol oxidase of *Brevibacterium sterolicum*: comparison with choA of *Streptomyces* sp. Gene. 103: 93–96

Porath J (1992). Immobilized metal ion affinity chromatography. Protein Exp. Purif. 3: 263-281.

Richmond W (1973). Preparation and properties of a cholesterol oxidase from Nocardia sp. and its application to the enzymatic assay of total cholesterol in serum. Clin. Chem. 19: 1350–1356.

Richmond W (1992). Analytical reviews in clinical biochemistry: the quantitative analysis of cholesterol. Ann. Clin. Biochem. 29: 577–597.

Schönbrunn E, Eschenburg S, Luger K, Kabsch W, Amrhein N (2000). Structural basis for the interaction of the fluorescence probe 8-anilino-1-naphthalene sulfonate (ANS) with the antibiotic target MurA. Proc. Natl. Acad. Sci. USA. 97: 6345–6349.

Shao J, Xin Y, Li RX, Fan Y (2011). Vitreous and serum levels of transthyretin (TTR) in high myopia patients are correlated with ocular pathologies. Clin. Biochem. 44: 681-685.

Shirokano Y, Nakamura K, Mizusawa K (1977). Purification and some properties of an extracellular 3b-hydroxy steroid oxidase produced by *Corynebacterium cholesterolicum*. J. Ferment. Technol. 55: 337–346.

Slade D, Ferreira D, Marais JP (2005). Circular dichroism, a powerful tool for assessing absolute configuration of Natural Products. Phytochemistry, 66: 2177–2215

Sojo M, Bru R, Lopez-Molina D, Garcia-Carmona F, Argulles JC (1997). Cell-linked and extracellular cholesterol oxidase activities from Rhodococcus erythropolis, isolation and physiological characterization. Appl. Microbiol. Biotechnol. 47: 583–589.

Terpe K (2003). Overview of tag protein fusions: from molecular and biochemical fundamentals to commercial systems. Appl. Microbiol. Biotechnol. 60: 523–533.

Tomioka H, Kagawa M, Nakamura S (1976). Some enzymatic properties of 3b-hydroxy steroid oxidase produced by *Streptomyces violascens*. J. Biochem. 79: 903–915.

Uwajima T, Yagi H, Terada O (1974). Properties of crystalline 3b-hydroxysteroid oxidase of *Brevibacterium sterolicum*. Agric. Biol. Chem. 38: 1149–1156.

Wang LG, Wang W (2007). Coenzyme precursor-assisted expression of a cholesterol oxidase from *Brevibacterium* sp. in *Escherichia* coli. Biotechnol. Lett. 29: 761–766.

Xin Y, Yang HL, Xia XL, Zhang L, Cheng C, Mou GC, Shi J B, Han YF, Wang W (2011). Affinity purification of a cholesterol oxidase expressed in *Escherichia* coli. J. Chromatogr. B. 879: 853-858.